J. Fluid Mech. (1983), *vol.* 135, *pp.* 111–122
Printed in Great Britain

On the formation of vortex pairs near orifices

By P. BLONDEAUX AND B. DE BERNARDINIS
Istituto di Idraulica, Università di Genova

(Received 14 September 1982 and in revised form 7 February 1983)

A two-dimensional vortex pair is commonly generated by pushing fluid down a semi-infinite channel by means of an impulsively started piston. The strength and separation of the two fully developed vortices strongly depend upon the time history of the piston motion. When the piston is impulsively stopped, two secondary vortices are formed downstream of the channel ends and interact with the primary pair in a fairly complicated way.

In the present work we attempt to provide a discrete-vortex model of the process of pair formation. The effects of viscosity are assumed to affect only the separation process, having negligible influence on the overall flow. In the limit of infinite Reynolds number, the problem becomes one of inviscid flow, and the separation at the sharp edges is approximated by a Kutta–Joukowski condition, large vortex regions being replaced by simple concentrated vortices. The growing vortex sheets shed from the edge are represented by a simplified model due to Brown and Michael.

Present results are able to account for the failure of the 'puffing' technique as well as the success of Barker and Crow's 'downwash' technique in producing vortex pairs.

Flow-visualization experiments are also reported, and good qualitative agreement is found between numerical and experimental results.

The present model also shows that the presence of secondary vortices drastically modifies the trajectories of free vortices as obtained in a previous work due to Sheffield.

1. Introduction

A two-dimensional vortex pair is commonly generated by pushing fluid down a semi-infinite channel by means of an impulsively started piston. The flow separates at the sharp edges of the channel opening, and two free shear layers are shed which roll up into coherent spirals. Thus a vortex pair is formed which moves downstream with its self-induced velocity. The strength and separation of the two fully developed vortices strongly depend upon the time history of the piston motion. Barker & Crow (1977, hereinafter referred to as BC) succeeded in producing a vortex pair which propagated away from the opening when the flow in the channel was forced to decrease slowly after the formation of the pair. But they found that, by suddenly stopping the piston, vortices were created which appeared quickly to draw together and dissipate. They ascribed this failure to the inadequacy of the 'puffing' technique in supplying the necessary fluid to fill the recirculation cell.

The generation process can be divided into two parts. First, two vortices are formed, one at each edge. For an initial short time the growth of each vortex near the channel end can be related to the local form of the attached flow past an isolated sharp edge through a similarity law extensively discussed by Rott (1956), Graham (1977) and Pullin (1978). Soon, however, this local dependence breaks down as the effect of the opposite edge becomes significant and the rolling-up vortex sheet is

affected by the overall flow (Pullin 1978; Pullin & Perry 1980). During the second part of the process the geometric shape of the generating channel exercises a strong influence on the trajectories of the two vortices just formed.

Sheffield (1977), bypassing the analysis of the generation process, calculated the trajectories of an ideal vortex pair near channel openings of different shapes. By using conformal-transformation theory and applying Routh's theorem, he found that the two vortices will not travel back into the channel provided that their initial positions lie outside a region adjacent to the wall and bound by two limiting trajectories. We also infer from Sheffield's results that vortices do not collide and break up near the axis of symmetry only in the case when the distance of the vortex pair from the channel edges is very large.

This may suggest a criterion for obtaining vortex pairs which are able to travel far downstream. However, Kelvin–Helmholtz instability of the free layers and transition into turbulence may be expected to occur if the generation process takes too long a time. On the other hand, if the piston is stopped suddenly, we find that two secondary vortices are shed from the separation edges and interact with the primary pair in a fairly complicated way (figure 1).

The latter phenomenon does not occur in BC's 'downwash' technique. Pullin & Perry (1980) recently illustrated the growth of a double-layer secondary vortex and the formation of a near-wedge vortex pair. Analogies exist between the plane and the axisymmetric cases. Maxworthy (1977) and Didden (1979), in their experiments on the generation of vortex rings by the 'puffing' technique, found that the diameter of the ring decreased moving downstream, and suggested that this behaviour was caused by the presence of a secondary vortex ring as well as that of the solid walls.

In the present work we attempt to provide a point-vortex model of the process of pair formation and a general extension of Sheffield's results.

It is assumed that viscous effects are significant only during the separation process and have negligible influence on the overall flow. In the limit of infinite Reynolds number, the problem becomes one of inviscid flow, and the separation at the sharp edges is approximated by a Kutta–Joukowski condition, large vortex regions being replaced by simple concentrated vortices. The growing vortex sheets shed from the edge are represented by a simplified model due to Brown & Michael (1954).

The latter, used by Rott (1956) and Graham (1977), is attractive for its simplicity and ability to give good qualitative results. However, as Pullin (1970) and Graham (1977, 1980) pointed out, details of the flow near the sharp edge and of the growing spiral are not properly represented.

We apply the above model to study (*a*) the trajectories of two free vortices released symmetrically near the channel wall far from the opening of a semi-infinite channel when growing secondary vortices are present, and (*b*) the generation of vortices by two types of outflow from the channel ('puffing' and 'downwash' technique). Flow-visualization experiments have been performed in order to check the numerical calculations.

2. Theory

We consider a two-dimensional channel of width $2D$. The walls are parallel plates of negligible thickness whose ends are two sharp edges of zero internal angle (figure 1). Symmetry implies that the axis of the channel is a streamline. Thus, if the axial plane is replaced by a wall, the problem is reduced to one where only a single sharp

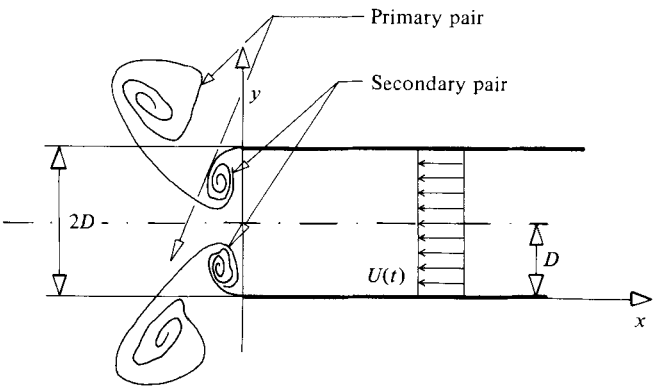

FIGURE 1. The wall geometry.

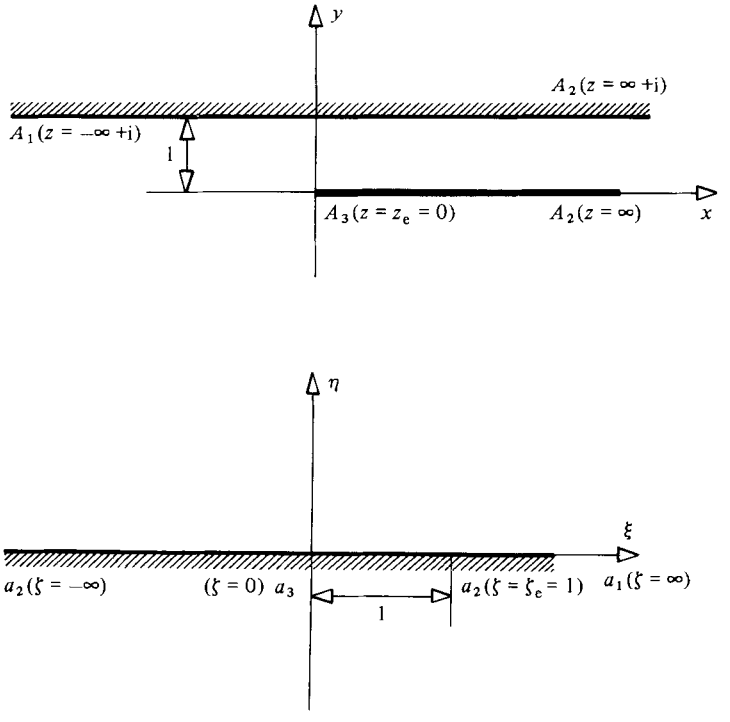

FIGURE 2. Schwartz–Christoffel transformation of the physical z-plane to the upper-half ζ-plane.

edge is present. We assume a Cartesian coordinate system (x, y) with the origin at the lower edge of the opening and the x-axis coincident with the channel wall as shown in figure 2. Choosing D as the unit of length and using a Schwartz–Christoffel transformation, the function f given by

$$z = f(\zeta) = -\frac{1}{\pi}[\zeta + \ln(\zeta - 1)] + \mathrm{i} \tag{1}$$

is found such that the interior of the channel in the physical z-plane ($z = x + \mathrm{i}y$) is

mapped onto the upper half of the complex ζ-plane ($\zeta = \xi + \mathrm{i}\eta$). In particular, the salient edge $z_e = 0$ is mapped onto the origin of the ζ-plane (figure 2).

2.1. *Sheffield's problem*

We first examine Sheffield's problem and calculate the trajectory of a free vortex of constant positive (counterclockwise) strength Γ_1 approaching the channel opening, from a point far 'upstream' near the wall.

The attached flow, associated with the presence of the point vortex, separates at the sharp edge and gives rise to the shedding of a vortex sheet. The latter rolls up into a concentrated vortex, which we shall refer to as the secondary vortex and assume can be represented by a single growing point vortex $\Gamma_2(t)$ at $z_2(t)$ plus a cut joining it to the edge as in the simplified model first suggested by Brown & Michael (1954). In the transformed plane the complex potential $W(\zeta)$ due to the primary and secondary vortex and their images is

$$W(\zeta) = \sum_{k=1}^{2} \frac{\mathrm{i}\Gamma_k}{2\pi} \ln \frac{\zeta - \zeta_k}{\zeta - \bar{\zeta}_k}, \tag{2}$$

where the explicit time dependence has been suppressed for convenience. In order to determine the vortex velocity in the z-plane, Routh's rule must be used. We find that, at the position z_j of the jth vortex,

$$\left[\frac{\mathrm{d}W}{\mathrm{d}z}\right]_{z=z_j} = \frac{1}{f(\zeta_j)} \left\{ q_j - \frac{\mathrm{i}\Gamma_j}{2\pi} \left[\frac{1}{\zeta_j - \bar{\zeta}_j} + \frac{f''(\zeta_j)}{2f'(\zeta_j)} \right] \right\}, \tag{3a,b}$$

where

$$q_j = \sum_{\substack{k=1 \\ k \neq j}}^{2} \frac{\mathrm{i}\Gamma_k}{2\pi} \left[\frac{1}{\zeta_j - \zeta_k} - \frac{1}{\zeta_j - \bar{\zeta}_k} \right].$$

The equation of motion of the vortex being shed from the edge can be obtained by imposing the condition of zero total force on the vortex plus the cut $z_2(t) - z_e$. This leads to the following modified zero-force equation (Rott 1956; Graham 1977, 1980) in the transformed plane:

$$\frac{\partial \zeta_j(t)}{\partial t} \Gamma_j(t) + \frac{f(\zeta_j) - f(0)}{f'(\zeta_j)} \frac{\partial \bar{\zeta}_j(t)}{\partial t} - \Gamma_j(t) \left[\frac{\mathrm{d}\bar{W}}{\mathrm{d}z} \right]_{z = z_j(t)} \frac{1}{f'(\zeta_j)} = 0, \tag{4}$$

where $j = 2$ for the present case.

As in Brown & Michael's model, the singularity at the sharp edge is eliminated by applying the Kutta–Joukowski condition in the transformed ζ-plane:

$$\left[\frac{\mathrm{d}W}{\mathrm{d}\zeta}\right]_{\zeta=0} = 0. \tag{5}$$

The equation of motion for the free point vortex, which is force-free and moves with the fluid, is

$$\frac{\partial \bar{\zeta}_1}{\partial t} = \left[\frac{\mathrm{d}\bar{W}}{\mathrm{d}z} \right]_{z=z_1} \frac{1}{f'(\zeta_1)}. \tag{6}$$

The trajectories have been determined by numerical integration of (4)–(6) by means of the Runge–Kutta–Gill method.

The initial position $z_1(0)$ of the free vortex is chosen outside the channel ($y_1(0) < 0$) and far enough from the edge ($x_1(0) \gg |y_1(0)|$) so that the initial vortex path is parallel to the wall and the flow induced around the edge is very weak. The growing secondary

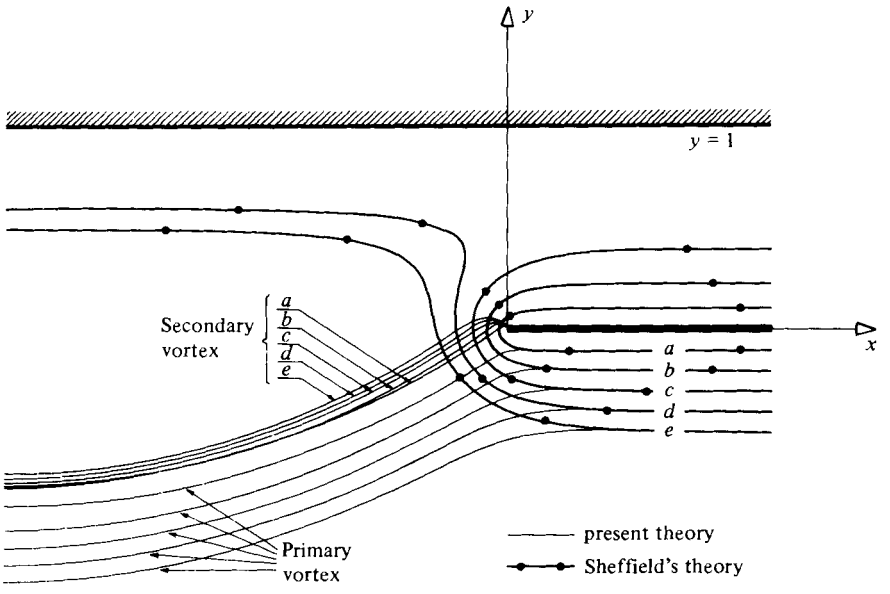

FIGURE 3. Sheffiield's problem. Trajectories of a free vortex obtained with (present theory) or without (Sheffield's theory) the presence of a growing secondary vortex. Initial positions: (*a*) $z_1(0) = 10-0.1\mathrm{i}$; (*b*) $z_1(0) = 10-0.2\mathrm{i}$; (*c*) $z_1(0) = 10-0.3\mathrm{i}$; (*d*) $z_1(0) = 10-0.4\mathrm{i}$; (*e*) $z_1(0) = 10-0.5\mathrm{i}$.

vortex is introduced after a very small time interval δt, when the rolling-up process has just started very near the sharp edge. The initial values of its total circulation $\Gamma_2(\delta t)$ and its position $z_2(\delta t)$ can be obtained by similarity solutions of (4) and (5) (see Graham 1977).

The integration time step Δt was chosen so that the local relative error was less than 10^{-4}.

Figure 3 shows some of the trajectories of the primary and secondary vortices obtained by the above procedure for different initial values of $z_1(0)$.

The striking feature emerging from the results is that neither of the two vortices moves back into the channel. The initial trajectory of the primary vortex is parallel to the wall and unaffected by the presence of a weak and almost stationary secondary vortex. The latter starts growing very quickly only when the primary vortex travels inside a near-edge region of order $y_1(0)$. When the two vortices reach the same strength, they form a pair which convects away from the sharp edge at a large angle (of about 30°) to the centreline wall along a nearly straight path. Also shown in figure 3 are the trajectories of the free vortex predicted by Sheffield's theory for the same set of initial values of z_1.

2.2. *The problem of the generation of vortex pairs*

The generation of vortex pairs is now investigated. An impulsively started and stopped slug flow $U(t) = \hat{U}[H(t)-H(t-T_f)]$ is imposed in the channel and represented in the transformed plane by a source of time-varying strength $m(t) = 2U(t)/\hat{U}$ at the point $\zeta = 1$. If the velocity scales on the maximum flow velocity $\hat{U}$ while D again acts as the lengthscale, the complex potential is given by

$$W_b(\zeta) = \frac{m}{2\pi}\ln(\zeta-1). \tag{7}$$

As the flow in the channel starts, a vortex sheet is shed from the sharp edge and starts to roll up. We use the Brown & Michael model again to describe it. The strength $\Gamma_1(t)$ and position $z_1(t)$ of the growing point vortex are obtained from the numerical integration of (4) and (5) with $j = 1$ and of (3), where q_j is now given by the following relationship:

$$q_j = \frac{\mathrm{d}W_\mathrm{b}}{\mathrm{d}\zeta}. \tag{8}$$

When the flow has just been set into motion, a flow pattern develops within a small region around the end of the channel wall and shows features similar to that of the case of singular attached flow past an infinite wedge.

The complex velocity in this 'inner' region may be expressed in the general form

$$\frac{\mathrm{d}W_\mathrm{e}}{\mathrm{d}z} = u - \frac{\mathrm{i}v}{2z^{\frac{1}{2}}}, \tag{9}$$

where u is given by $\hat{u}t^\beta$ and v by $\hat{v}t^\alpha$. The real functions of time u and v describe the symmetrical and asymmetrical components of velocity, and are determined by a matching condition with the 'outer' flow in the form

$$\lim_{z \to z_\mathrm{e}} \overline{\frac{\mathrm{d}W}{\mathrm{d}z}} = \frac{\mathrm{d}W_\mathrm{e}}{\mathrm{d}z}. \tag{10}$$

Graham (1977) showed that (4) and (5) admit a similarity solution. If α, β and $\hat{u}$ are zero

$$\Gamma_1(t) \sim v^{\frac{4}{3}} t^{\frac{1}{3}}, \quad x_1(t) = 0, \quad y_1(t) \sim (vt)^{\frac{2}{3}}; \tag{11a–c}$$

whereas if, for example, at small time $|\hat{u}| \gg |\hat{v}|$, $\beta = 0$ but $\alpha = 1$, the solution is

$$\Gamma_1(t) \sim u^{\frac{1}{2}} v t^{\frac{1}{2}}, \quad x_1(t) \sim ut, \quad y_1(t) = 0. \tag{12a–c}$$

By substituting from the expressions for W and W_e into (10) one can show that the presence of the wall at $y = 1$ gives rise to a weak symmetrical component of velocity.

Thus for $|u| < |v|$ we expect from (11) and (12) that, for small t, the leading-order terms of the solution may be put in the form

$$\Gamma_1 \sim v^{\frac{4}{3}} t^{\frac{1}{3}}, \quad x_1 \sim ut, \quad y_1 \sim (vt)^{\frac{2}{3}}, \tag{13a–c}$$

the x-term being of higher order than the y-term.

Figure 4 shows numerical results which confirm that the above approximation is sensible.

At $t = T_\mathrm{f}$ the slug flow is impulsively stopped so that the growth of the primary vortex is interrupted suddenly, while a secondary vortex starts to develop.

In the numerical approach the primary vortex is then modelled as a free point vortex of constant strength $\Gamma_1(T_\mathrm{f})$, and its motion is described by (6). The Brown & Michael model is applied to analyse the growth of the secondary vortex, whose strength $\Gamma_2(t)$ and position $z_2(t)$ are given by (3)–(5).

Numerical calculations over a large range of flow durations have shown the existence of two different flow regimes. For $T_\mathrm{f} < 5$ the primary vortex, which remains in the near-edge region during its growth, and the secondary vortex quickly form a pair which approaches the midline wall. After following a fairly straight path they spread apart, the first vortex propagating away, the second moving back into the channel. For $T_\mathrm{f} > 5$ this pairing process is not present and the trajectory of the

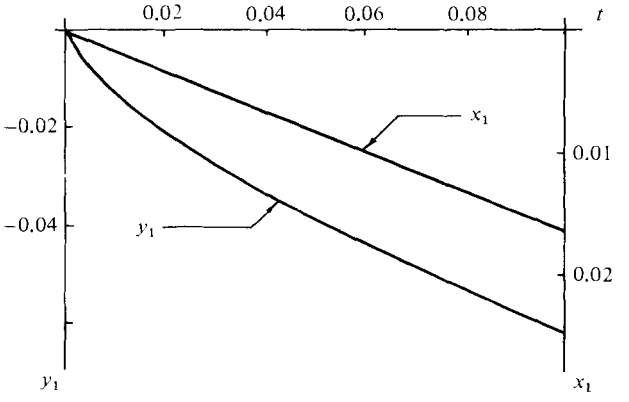

FIGURE 4. Vertical and horizontal position of the primary vortex centre versus time within the initial period of the generation process.

primary vortex is mainly influenced by the midline wall representing the effect of the vortices on the other side of the channel. The secondary-vortex growth is weaker than in the former regime although its trajectory remains almost unchanged. These flow patterns appear in figure 5, where the results of the calculations for different values of T_f are shown along with the trajectories of the primary vortex for $t > T_f$, obtained by assuming $\Gamma_1(t) = \Gamma_1(T_f)$ and ignoring the existence of the secondary vortex as in Sheffield's theory.

The 'puffing' technique is found to cause a consistent reduction of the distance between the fully developed vortex and the midline wall in agreement with BC's and Didden's (1979) experimental results. This reduction in turn causes finite-core vortices either to undergo irreversible changes or, for short T_f, to collide; in both cases preventing them from propagating far away. In contrast pairs obtained by BC exhibit a separation larger than the opening width, this being due to the 'downwash' technique, which allows the flow to slowly decelerate and inhibits the growth of the secondary vortex.

The mathematical model developed in this paper can be easily adapted to study the process of BC's technique. The velocity $U(t)$ is not instantaneously set to zero at $t = T_f$, but allowed to decrease in time in such a way that the basic attached flow at the sharp edge cancels out the singular velocity component induced by the primary vortex.

So the strength $m(t)$ of the source in the transformed plane is assumed to be constant for $0 < t \leqslant T_f$, and is calculated for $t > T_f$ by requiring that

$$m(t) = -2\Gamma_1(T_f)\frac{\mathrm{Im}\,(\zeta_1(t))}{|\zeta_1(t)|^2}. \tag{14}$$

Figure 5 shows that for $0 < t \leqslant T_f$ the trajectory of the growing vortex is identical with that obtained by the 'puffing' technique. At $t = T_f$ the feeding cut is suddenly eliminated, and for $t > T_f$ no more vorticity is shed from the sharp edge because of the condition expressed by (14). So no secondary vortex is formed and the primary vortex moves freely with the local velocity due to the channel outflow and its image.

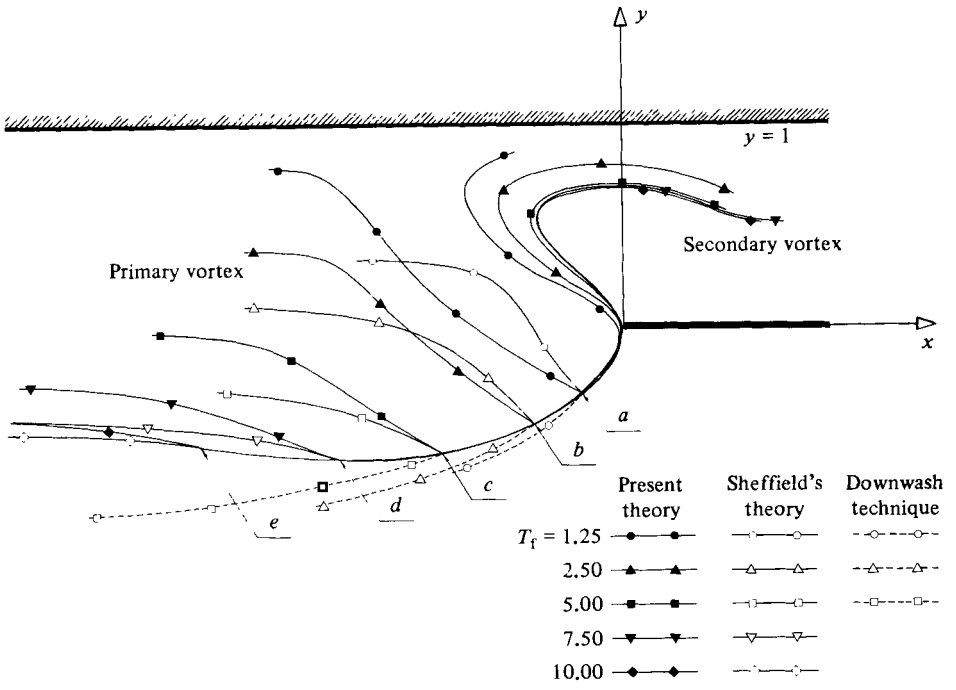

FIGURE 5. Vortex-pair generation by 'puffing' and 'downwash' techniques. Prediction obtained by the present theory compared with Sheffield's theory applied to the primary vortex for $t > T_f$ and with initial positions: (*a*) $T_f = 1.25$, $z_1(T_f) = -0.21 - 0.31i$; (*b*) $T_f = 2.5$, $z_1(T_f) = -0.43 - 0.45i$; (*c*) $T_f = 5.0$, $z_1(T_f) = -0.88 - 0.60i$; (*d*) $T_f = 7.5$, $z_1(T_f) = -1.37 - 0.63i$; (*e*) $T_f = 10.0$, $z_1(T_f) = -1.90 - 0.59i$.

3. Experiments

The experimental apparatus, shown schematically in figure 6, consisted of a water channel with a rectangular cross-section 2.5 cm high and 1.0 cm wide. At the upstream end of the channel the lower wall was joined to the bottom of a reservoir, while the upper wall ended with a sharp edge of 5° internal angle.

A rectangular piston, driven through a gear-box by a high-torque stepping motor, created the basic slug flow. The motor was operated via a logic control circuit, and a constant speed could be obtained over most of the piston stroke, providing high initial acceleration. The piston was stopped impulsively at $T_f = \hat{U}/L$, where $\hat{U}$ is the velocity of the piston and L is the displacement.

The flow details were visualized by blue dye injected near the sharp edge by a capillary tube. The motion of the vortices was filmed on a 16 mm coloured ciné film at 24 frames/s. Runs were performed for $T_f = 3.0$, 5.5 and 10.0 and $R_c = 390$ and 1100, where $R_c = \hat{U}D/\nu$ and ν is the kinematic viscosity. The trajectories of the primary and secondary vortex cores were obtained by a frame-by-frame analysis of the ciné film.

In figure 7 the vortex trajectories averaged over four different runs are compared with the corresponding numerical results.

As may be seen from figures 8(*a*, *b*) (plate 1), showing the nearly formed vortex pair for $T_f = 3.0$ and 10.0, the cores of the vortices are not well defined; thus they have been inferred by inspection from the observed pattern of the vortex streaklines.

Several authors investigating the rolling-up process of starting vortices (Pierce

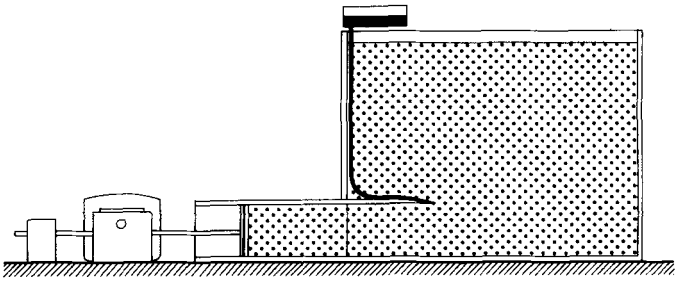

FIGURE 6. Experimental set-up.

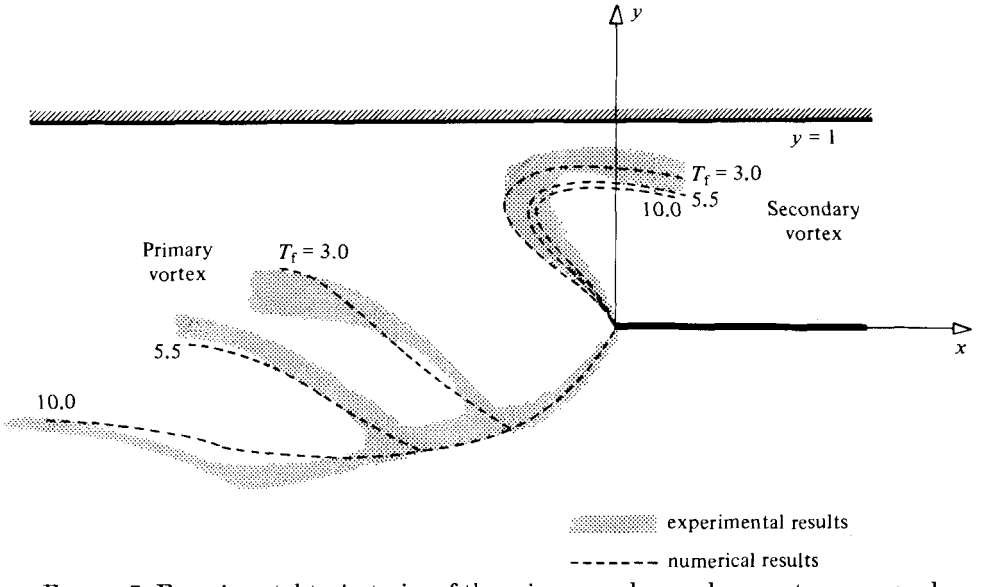

FIGURE 7. Experimental trajectories of the primary and secondary vortex compared with the present-model prediction.

1961: Pullin & Perry 1980; BC) have observed the concentration of streaklines around a series of apparent rotation centres. This is a salient feature of figure 8(*c*). However, once the level of vibrations present in the apparatus was reduced, the phenomenon disappeared as shown in figure 8(*d*).

BC assumed that such a behaviour of the streaklines represents the development of 'discrete vortices' on the vortex sheet and the start of transition to turbulence. They observed that the above pattern is apparently similar to that occurring on a free shear layer undergoing Kelvin–Helmholtz instability as observed by Brown & Roshko (1974) and postulated that it may be the final stage of the growth of unstable disturbances within an annular region surrounding the vortex core where viscous diffusion smooths out the vorticity distribution. However, Crow's (1975) analysis does not apply directly to the present flow, since the effects of the outer discrete spiral structure of the vortex is not included and starting vortex sheets have been found to be stable at least against short-wave disturbances. Two combined stabilizing effects are present: the thickness (Dhanak 1981) and the stretching (Moore 1976) of the shear layer throughout the rolling-up process. Therefore, when short waves exist within the shear layer, they remain bounded for all time and a great deal of caution must be

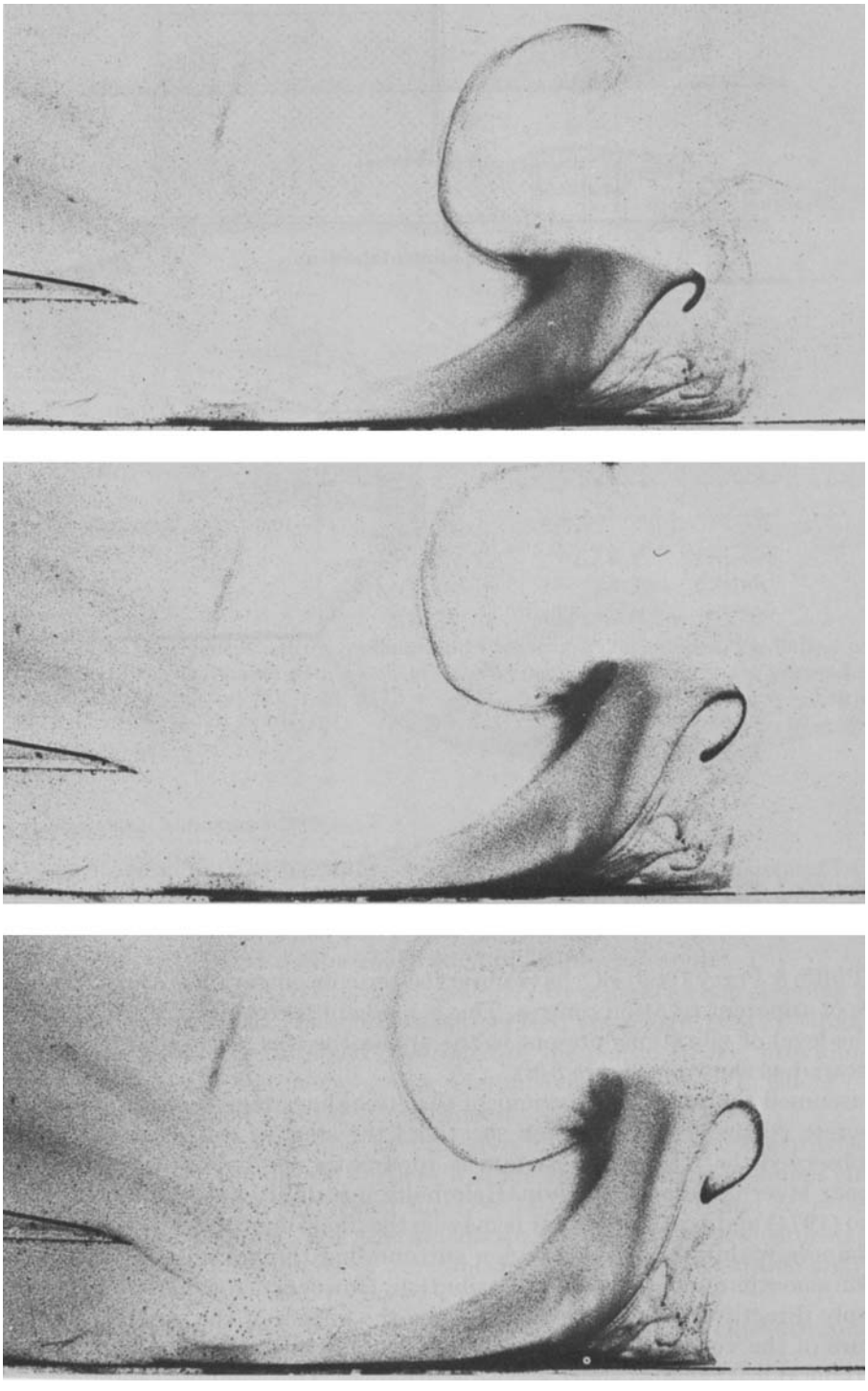

FIGURE 9. Photos of dye in water showing the rolling up of the free shear layer generated by smooth wall separation of the boundary layer underneath the primary vortex.

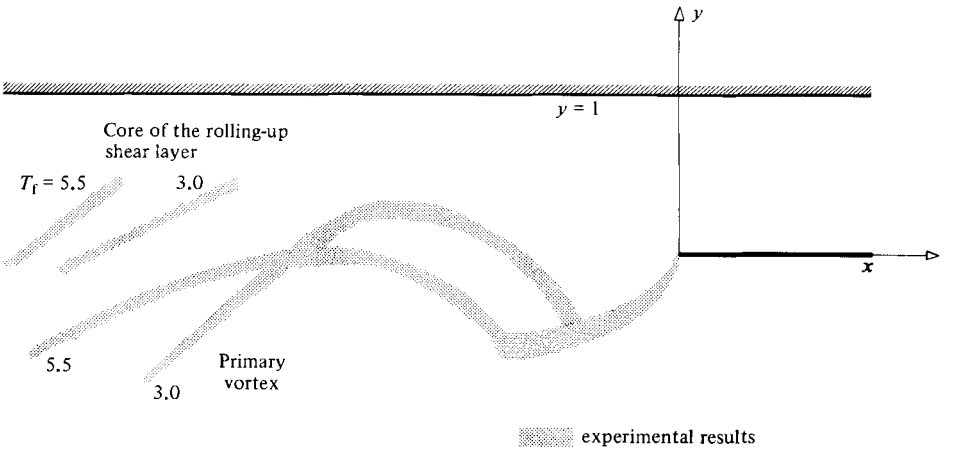

FIGURE 10. Experimental trajectories of the primary vortex and of the core of the rolling-up shear layer generated by smooth wall separation of the boundary layer.

exercised in interpreting the streakline behaviour (Pullin & Perry 1981). Hama (1962) analysed the case of a shear flow perturbed by an unamplified travelling sinusoidal wave. He showed that the streakline that emerges from the critical layer always appears to roll up regardless of the true nature of the superposed perturbation. On the basis of the previous remarks we may conclude that the presence of discrete vortices cannot be positively identified, and transition to turbulence does not occur.

The experimental results did not show any appreciable Reynolds-number dependence, and they were found to be in reasonable quantitative agreement with potential-flow theory. This works quite well provided that the correct circulation distribution is maintained.

The formation of vortex pairs obtained by 'puffing' fluid out of a symmetric channel is fully represented by the present experimental apparatus. However, the presence of a midline wall on which a laminar boundary layer grows with thickness $O[(\nu t)^{\frac{1}{2}}]$ may affect the overall flow. Indeed, when the primary and secondary vortex start spreading apart, the boundary layer separates and two cells of recirculating flow appear to move along the wall underneath the vortices. The largest eddy is found to occur to the right of the primary vortex (figure 8*b*). It develops very rapidly and leaves the wall when the local thickness of the boundary layer grows dramatically.

Then the eddy is ejected into the inviscid region, where it is rapidly convected away, leaving behind a free shear layer shed from the separation point at the wall. The latter rolls up into a strong eddy, which interacts with the primary vortex and causes it to move away from the midline wall as shown in figure 9. The displacement effect is easily depicted from the trajectory of the primary vortex (figure 10). The above observations are fully in agreement with Harvey & Perry's (1971) wind-tunnel experimental results and with Walker's (1978) numerical predictions. They also confirm the implications of Saffman's (1979) inviscid theory.

4. Conclusion

The Brown & Michael (1954) model appears to describe satisfactorily the generation process of two-dimensional vortex pairs obtained by pushing fluid down a semi-infinite channel.

Numerical results showed that the trajectories and the persistency of the just-formed pair strongly depend upon the presence of secondary vortices, which also explain the failure of the 'puffing' technique as well as the success of the 'downwash' technique.

A quantitative comparison between theoretical and experimental trajectories of pairs obtained by the 'puffing' technique showed a fairly good agreement, till the stage when a bouncing effect is produced which is caused by the separation of the wall boundary layer and the formation of a free shear layer.

The authors are grateful to Dr M. R. Dhanak, Dr J. M. R. Graham and Dr G. Seminara for their advice and discussion on various issues arising from the work.

REFERENCES

BARKER, S. J. & CROW, S. C. 1977 The motion of two-dimensional vortex pairs in a ground effect. *J. Fluid Mech.* **82**, 659.

BROWN, C. E. & MICHAEL, W. H. 1954 Effect of leading edge separation on the lift of a delta wing. *J. Aero. Sci.* **21**, 690.

BROWN, G. L. & ROSHKO, A. 1974 On density effects and large structure in turbulent mixing layers. *J. Fluid Mech.* **64**, 775.

CROW, S. C. 1975 The stability of vortex cores. *Poseidon Res. Note* 4.

DHANAK, M. R. 1981 The stability of an expanding circular vortex layer. *Proc. R. Soc. Lond.* **A375**, 443.

DIDDEN, N. 1979 On the formation of vortex rings. *Z. angew. Math. Phys.* **30**, 101.

GRAHAM, J. M. R. 1977 Vortex shedding from sharp edges. *Imperial College Aero. Rep.* 77.06.

GRAHAM, J. M. R. 1980 The forces on sharp-edged cylinders in oscillatory flow at low Keulegan–Carpenter numbers. *J. Fluid Mech.* **97**, 331.

HAMA, F. R. 1964 Streaklines in a perturbed shear flow. *Phys. Fluids* **5**, 664.

HARVEY, J. K. & PERRY, F. J. 1971 Flow field produced by trailing vortices in the vicinity of the ground. *AIAA J.* **9**, 1659.

MAXWORTHY, T. 1977 Some experimental studies of vortex rings. *J. Fluid Mech.* **81**, 465.

MOORE, D. W. 1976 The stability of an evolving two-dimensional vortex sheet. *Mathematika* **23**, 35.

PIERCE, D. 1961 Photographic evidence of the formation and growth of vorticity behind plates accelerated from rest in still air. *J. Fluid Mech.* **11**, 460.

PULLIN, D. I. 1978 The large-scale structure of unsteady self-similar rolled-up vortex sheets. *J. Fluid Mech.* **88**, 401.

PULLIN, D. I. & PERRY, A. E. 1980 Some flow visualization experiments on the starting vortex. *J. Fluid Mech.* **97**, 239.

ROTT, N. 1956 Diffraction of a weak shock with vortex generation. *J. Fluid Mech.* **1**, 111.

SAFFMAN, P. G. 1979 The approach of a vortex pair to a plane surface in inviscid fluid. *J. Fluid Mech.* **92**, 497.

SHEFFIELD, J. S. 1977 Trajectories of an ideal vortex pair near an orifice. *Phys. Fluids* **20**, 543.

WALKER, J. D. A. 1978 The boundary layer due to a rectilinear vortex. *Proc. R. Soc. Lond.* **A359**, 167.

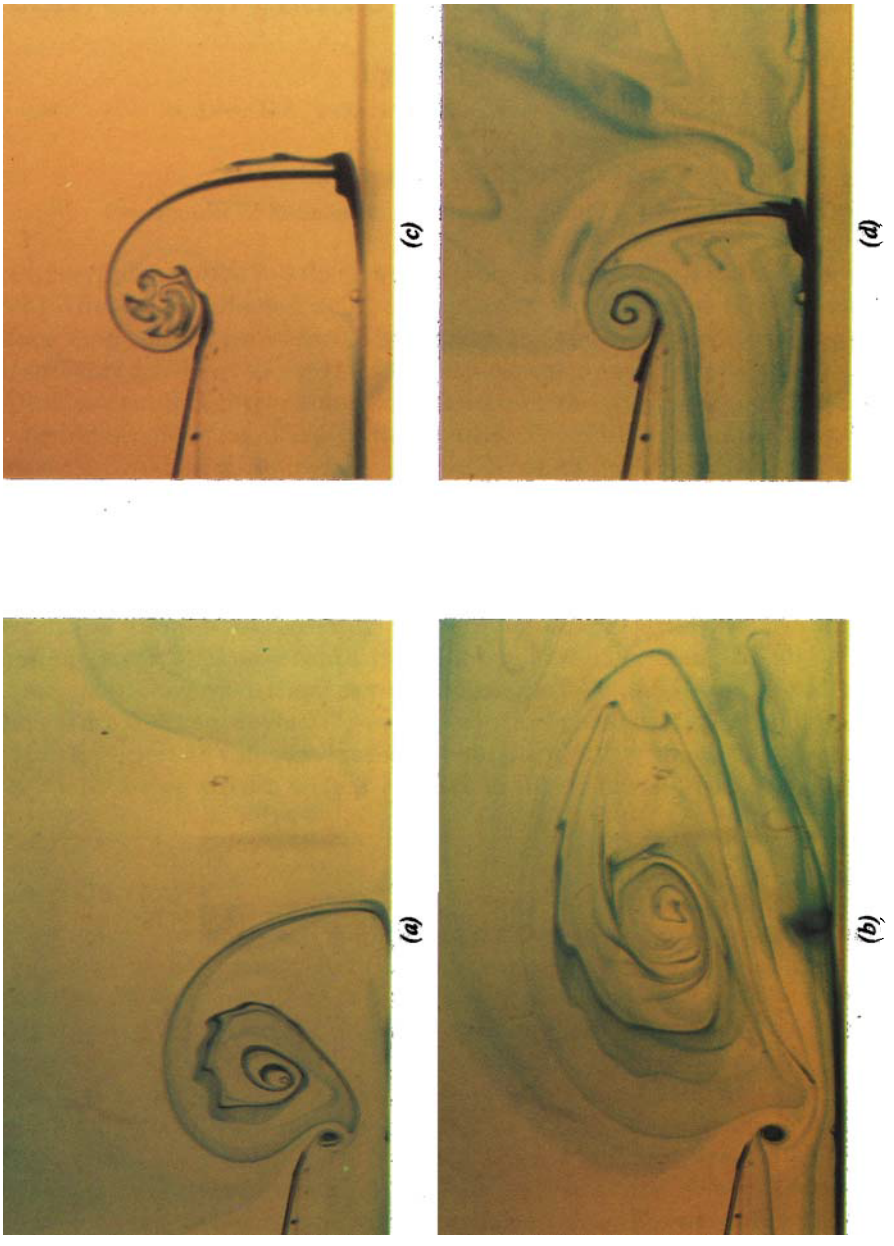

FIGURE 8. Photos of flow-visualization experiments. Secondary-vortex generation when the flow stops at *(a)* $T_f = 3.0$ and *(b)* $T_f = 5.5$. The rolling up of the vortex sheet during the generation of the primary vortex with *(c)* and without *(d)* the concentration of the streak lines around the apparent rotation centres.